New Trends in Nanoscale Mechanics of Nanostructures, Graphene Sheets and Nanocomposites

Editor's Notes

Vasyl Harik

Abstract Editor's notes first introduce special examples of nanostructures to illustrate a useful nanoscale homogenization criterion. Later editor's notes introduce chapters on graphene sheets, nanocomposites, molecular modeling of nanocomposites and new analysis of safety of carbon nanotubes along with reviews of new studies and applications. A review of a new registry matrix analysis and a nanoscale analog of the Newton's friction law are presented in chapter "Nanomechanics of Graphene Sheets: Registry Matrix Analysis and Interfacial Sliding" along with examples of interfacial sliding of the adjacent graphene sheets. Enhancement of material properties of nanocomposites and their molecular modeling analysis are lucidly presented in chapter "Molecular Mechanics of Polymer Nanocomposites". A new parametric map for geometric parameters of carbon nanotubes and different types of phagocytosis is presented to improve understanding of safety issues in nanotechnology (see chapter "Carbon Nanotubes and Safety," which points out the growing importance of safety in nanotechnology).

V. Harik (✉)
Nanodesigns Consulting, P.O. Box 5303, Wilmington, DE 19808-5303, USA
e-mail: Harik@nanodesignconsult.com

Introduction

Nanostructured materials such as graphene sheets and nanocomposites are important materials for the latest developments in nanotechnology. This part of the edited volume introduces some novel applications of graphene sheets (see chapter "Nanomechanics of Graphene Sheets: Registry Matrix Analysis and Interfacial Sliding") and the carbon nanotube based polymer composites (see chapter "Molecular Mechanics of Polymer Nanocomposites"). Advances in nanomechanics of graphene sheets (Fig. 1) are illustrated in chapter "Nanomechanics of Graphene Sheets: Registry Matrix Analysis and Interfacial Sliding" by reviewing new methods to control nanoscale sliding of graphene sheets through the registry matrix analysis of interfacial sliding of graphene sheets and a nanoscale analog of the Newton's friction law. The new *effect of the spatial exclusion of electrons (SEE)* during interaction between the spatially-distributed π–π electrons between the adjacent graphene sheets [1] is also reviewed in chapter "Nanomechanics of Graphene Sheets: Registry Matrix Analysis and Interfacial Sliding".

Material properties of graphene sheets have been discussed along with the nanoscale homogenization criterion for graphene sheets, carbon nanotubes and other nanostructures. The data of Fig. 2 can be used to illustrate this *homogenization criteria* [1]*, which requires at least ten smallest structural elements for the material properties to reach an invariant size-independent value, i.e., the macroscopic value*. This figure demonstrates that stability of nanorods increases along with their size. It also can be inferred from the data presented that the stability of such nanorods reaches its highest value as soon as their nanoscale structure becomes large enough to include the structural edge cell $(SEC)_{10}$ boundary characterized by a homogenization parameter $X_{10}(E)$. Here, $X_{10}(E) = 0.99$ indicating that a material property (i.e. formation energy) reaches the 99 % of its macroscopic value on the edge of a material consisting of 10 structural elements. The graphene flakes shown in Fig. 1 have not reached the critical size at which their material properties are independent of their size. This illustrates *the intrinsic nanoscale size dependence* of material properties below *the critical size of the ten structural elements or so*.

Fig. 1 Schematic of the two graphene lattices in a typical AAA stacking sliding from the incommensurate lattice-lattice registry (after [1])
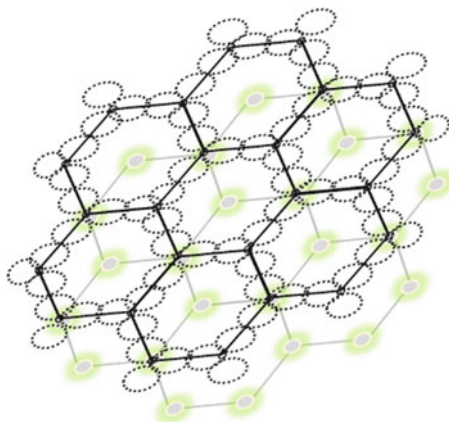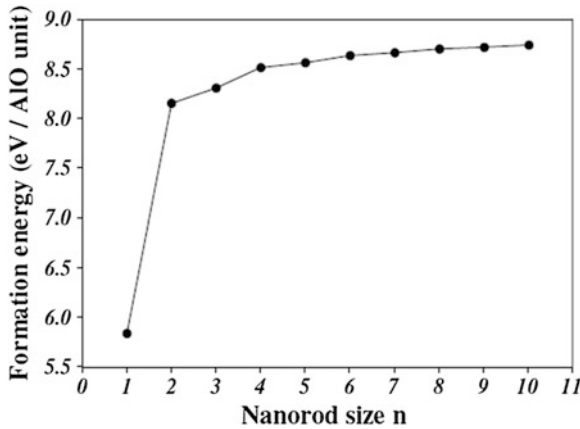
Fig. 2 Dependence of the formation energies of the nanorods as a function of the number of the so called $(AlO)_n$ units [2]. The limiting value of the formation energies is reached after 10 $(AlO)_n$ units on the structural edge boundary with a homogenization parameter $X_{10}(E) = 0.99$, which indicates the 99 % of the macroscopic value for the formation energy

Different materials with the distinct structural elements of varying intrinsic nanoscale properties have a unique $X_{10}(M)$ parameter for each material property, M. Hence, all material properties of a nanostructured material can be characterized by a set of homogenization parameters: $X_{10}(M_1)$, $X_{10}(M_2)$, $X_{10}(M_3)$ or by $X_9(M_1)$, $X_{12}(M_2)$, $X_{11}(M_3)$ and so on. Ideally, each nanostructured material should be characterized by pairs of homogenization parameters, $(X_{10}(M_1)$, $X_{11}(M_1))$, $(X_{10}(M_2)$, $X_{12}(M_2))$ or $(X_{10}(M_3)$, $X_{14}(M_3))$ and so on, where the value of the second homogenization parameter must be always unity, while the number of structural elements may vary for different materials and distinct material properties.

Nanoscale materials, which require less than 10 units to reach the macroscopic value of their material properties, exhibit strong intrinsic tendency to poses those properties. If a number of the minimum structural elements, which is required to reach the macroscopic value of material properties, is greater than 10 than a nanoscale material exhibits a weak intrinsic tendency to poses those properties. In Fig. 2 it is shown that nanorods exhibit intrinsic tendency for the formation energies, which is close to normal since $X_{10}(E) = 0.99$. When nanostructured materials include regions of the size, which is less that *the critical size* associated with the macroscopic properties (see Fig. 3), the material properties of these regions are highly dependent on their local dimensions and the ability to measure the size of distinct local material phases before the process of homogenization (i.e., volume averaging) or the local structural analysis with further multiscale analysis. Meng and Voyiadjis [3] have demonstrated such local regions along with very interesting laminar formations of the so called crystalline ZrN/AlN multilayer (Fig. 3).

The multiscale analysis of complex material systems shown in Fig. 3 can be quite challenging if the nanoscale measurements are not detailed enough or the

subsequent characterization of local and macroscopic material properties is lacking
a coherent framework of scaling parameters accompanied by appropriate ranges of
applicability of the local models used. In Fig. 3 the nanoscale scale of 2 nm has
been provided along with the modulation wavelength of material composition. In
Fig. 4 an example of multiscale modeling is presented for a material system of the
Si/Si_3N_4 nanopixel with the use of molecular dynamic (MD) modeling and the
finite element analysis (FEA), where the MD modeling region represents both
atoms and atomic bonds. Note that the MD region involving a graphene sheet is
smaller than the critical size of 10 structural elements consisting of carbon rings.
Such material system configuration may occur either by a necessity or as a result of
manufacturing (as in Fig. 3), which requires multiscale analysis such as shown in
Fig. 4.

   The multiscale modeling of interfacial regions in nanoscale material systems is
also very important for the carbon nanotube based nanocomposites. The use of MD
modeling region shown in Fig. 4 is important around embedded nanoscale fibers
and thick carbon nanotubes (Fig. 5). Chapter "Molecular Mechanics of Polymer
Nanocomposites" presents yet another method for multiscale modeling, i.e., Monte
Carlo based molecular mechanics modeling, which takes into account complex
molecular structure of interfacial regions in polymer nanocomposites with various
inclusions. Carbon nanotube based polymer nanocomposites represent an important
group of nanocomposites. The following editor's notes and chapter "Molecular
Mechanics of Polymer Nanocomposites" review some of the latest developments in
the nanoscale analysis of nanocomposites.
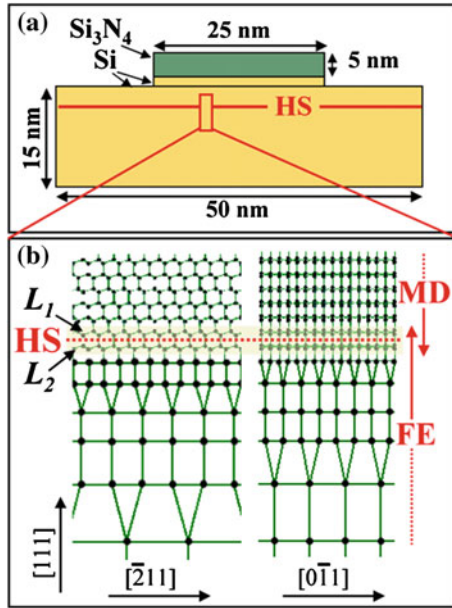
Fig. 4 a A schematic of the Si/Si₃N₄ nanopixel. The two dimensional projections shows Si₃N₄ and Si in *green* and *yellow*, respectively. Above and bellow the hand shake (HS) region (denoted by the *red line*), MD and FE apply respectively. **b** Close-up of the HS region and its surroundings in the Si substrate showing 2D views from two different directions. On the *top* is the MD region (*spheres* and *lines* represent atoms and atomic bonds), and on the *bottom* is the FE region (*spheres* and *lines* represent nodes and element boundaries). The *yellow box* marks the HS region in which particles are hybrid nodes/atoms, and the *red dotted line* marks the HS surface (after Voyiadjis, Aifantis and Weber [4])

Fig. 5 Axial stress distribution in polymer matrix: **a** perfect bonding, isostrain, **b** van der Waals bonding, isostrain (after Li and Chou [7])
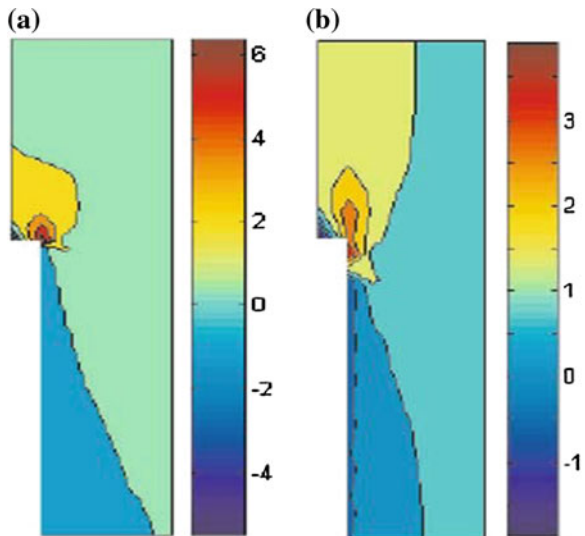
Carbon Inclusions in Polymer Matrix Nanocomposites

Polymer matrix nanocomposites are typically reinforced by carbon fibers, carbon nanotubes [5], graphene multilayers [6], flakes of graphene layers (Fig. 1), carbon nanofibers and other carbon inclusions. Chapter "Molecular Mechanics of Polymer Nanocomposites" shows examples of complex interface regions in polymer matrix nanocomposites, which may include gradients in material properties near interfaces, complex polymer networks and even interphases. In material systems, where there are small or insignificant gradients in material properties near interfacial surfaces, it is important to consider two limiting cases of a classical perfect interfacial bonding and a weak interfacial bonding [8] or the nanoscale weak bonding by van der Waals forces [7, 8]. For these types of cases Li and Chou [7] have used the so called structural molecular mechanics approach for the nanoscale finite element analysis of carbon nanotube polymer matrix composites (Fig. 5). In their study the stress distributions have been examined in the unit cell having the width, w, such that $w/R = 5$, where R is the radius of inclusion, R. They have shown that the stress concentration near the nanoscale inclusions with van der Waals bonding is lower than that near the perfectly bonded inclusions.

It should be mentioned that at nanoscale level there is no 100 % perfect bonding. There is a very strong covalent bonding between nanoscale inclusions and the structural elements of a matrix material. The covalent bonding or rather the high density covalent bonding is a close approximation for the perfect bonding in the classical sense. In practice, however, it is very hard to achieve the high density covalent bonding (Fig. 6). The density of covalent density at the interfaces depends on a number of factors such processing methods, chemical systems involved, local stoichiometry and the processing conditions. Nevertheless, the assumption of the perfect bonding is a very important and useful limiting case in the multiscale analysis of nanostructured materials.
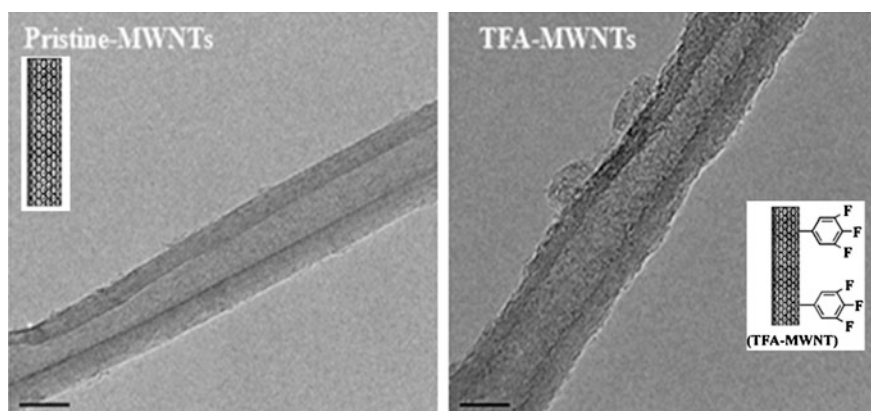

Fig. 6 Images of pristine and functionalized multiwall carbon nanotubes (MWNTs) by Trifluoroaniline (after [9]). Images are obtained by transmission electron microscope (TEM)

Nanoscale finite element analysis of Li and Chou [7] can also serve as a useful albeit limited guide (Fig. 5) for the case of nanocomposites with the semi-rectangular graphene platelets as reinforcing inclusions. One should remember the differences between the more confined case of cylindrical symmetry and the more open two-dimensional geometry. Chapter "Nanomechanics of Graphene Sheets: Registry Matrix Analysis and Interfacial Sliding" presents new results on interfacial properties of graphene sheets and the phenomena associated with the shearing deformation of graphene platelets of semi-rectangular form. Shearing deformation of nanoscale inclusions depends on nanoscale interfacial sliding between adjacent graphene sheets. Reinforcement of material properties in nanocomposites, which is reviewed in chapter "Molecular Mechanics of Polymer Nanocomposites", is affected by the interfacial properties and the molecular structure in the interfacial region near nanoscale inclusions. Interfacial phenomena are further discussed below and in all of the following chapters: for graphene sheets in chapter "Nanomechanics of Graphene Sheets: Registry Matrix Analysis and Interfacial Sliding", for polymer nanocomposites in chapter "Molecular Mechanics of Polymer Nanocomposites" and for the engulfment of carbon nanotubes in macrophages in chapter "Carbon Nanotubes and Safety". Safety of Nanotechnology is very important.

Carbon Nanotube/Polymer Interfaces in Nanocomposites

The nanotube/polymer interface plays an important role in the stress transfer in nanocomposites. The strength of interfacial adhesion depends on the surface area of the nanotube/polymer interface (see chapter "Molecular Mechanics of Polymer Nanocomposites"), its roughness (Fig. 6), interlocking of asperities and molecular bonding of the nanoscale interface [1, 8, 9]. Carbon nanotube surface can be modified by surfactants, nanoscale particles (e.g., oxide and nitride ceramics or graphene flakes) and the molecular chains capable of covalent bonding or van der Waals bonding by the aromatic units composed of carbon rings. Mechanical property measurements [10] of ceramic nanocomposites after the addition of 0.1 wt% of carbon nanotubes (CNTs) in the alumina have shown the increased fracture toughness by about 1.6 times from 3.7 to 4.9 MPa $m^{1/2}$. For 1 wt% CNTs/BaTiO$_3$ composite [10], the toughness value (1.65 MPa·$m^{1/2}$) is about 2.4 times than that of pure BaTiO$_3$ (0.68 MPa·$m^{1/2}$) (Fig. 7). Chapter "Nanomechanics of Graphene Sheets: Registry Matrix Analysis and Interfacial Sliding" presents a review of nanoscale sliding properties of graphene flakes, which also can improve toughness properties of the fiber-reinforced ceramic matrix nanocomposites by tailoring their layered interfacial properties.
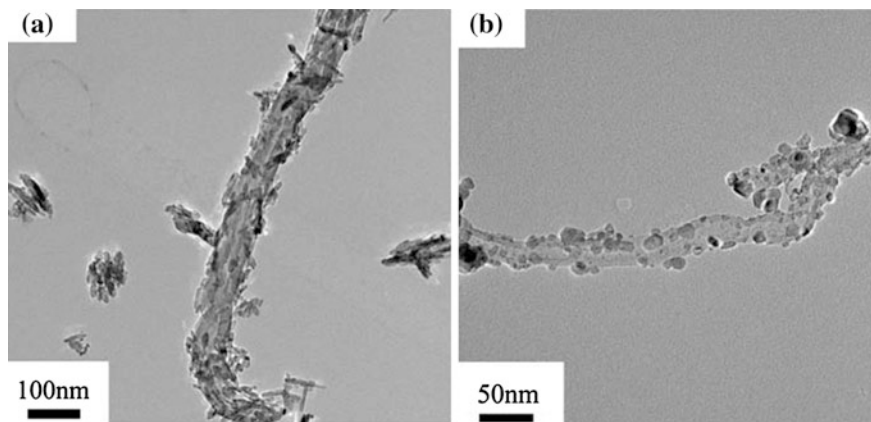
Fig. 7 TEM image of **a** rod-like TiO$_2$ nanoparticles on a carbon nanotube (CNT) and **b** tiny TiO$_2$ nanoparticles on CNTs (after [10])

## *Molecular Modeling of the Carbon Nanotube/Polymer Interfaces*

Molecular modeling of the carbon nanotube/polymer interfaces allows to examine nanoscale surface interactions at more details. Chapter "Nanomechanics of Graphene Sheets: Registry Matrix Analysis and Interfacial Sliding" introduces new results in nanomechanics of graphene sheets, which are used both for nano-scale electronic devices and for nanocomposites with polymer and ceramic matri-ces. The following examples of novel methods to tailor interfacial properties on molecular level are presented here to motivate both chapters "Nanomechanics of Graphene Sheets: Registry Matrix Analysis and Interfacial Sliding" and "Molecular Mechanics of Polymer Nanocomposites", where molecular modeling is used to enhance material properties of nanocomposites. Figures 8 and 9 illustrate molecular modeling of the non-covalent and covalent adsorption of alanine and alanine rad-icals onto the surface of a (5, 0) zig-zag single-walled carbon nanotube using the first principles calculations [11]. The π-electron interactions have been shown to play a significant role in the non-covalent absorption with the functional group close to the carbon nanotube surface naturally has a significant influence on the binding strength and the associated interactions.

Results of non-covalent functionalization of carbon nanotubes with alanine have shown that such functionalization enhances the conductivity of a (5, 0) zig-zag nanotube [11]. In the case of covalent adsorption of alanine radicals onto the surface of a carbon nanotube, the alanine-nanotube binding energy depends on the local lattice configuration at an adsorption site and on the type of electronegative atom (e. g., a strong amine group) that binds with the nanotube. Chapter "Nanomechanics of Graphene Sheets: Registry Matrix Analysis and Interfacial Sliding" presents other methods of analysis of different lattice configurations in the surface-surface sliding
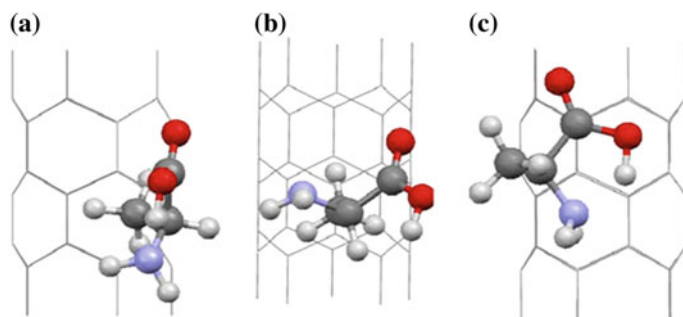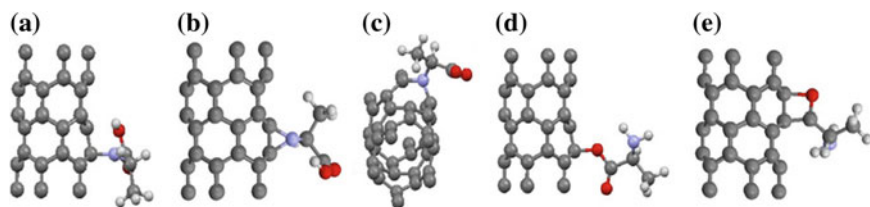
Fig. 8 Noncovalent adsorption of alanine on a (5, 0) zig-zag carbon nanotube (CNT): **a** $C_{50}ACH_3$-I, **b** $C_{50}ACH_3$-II and **c** $C_{50}ANH_2$-I (after [11])
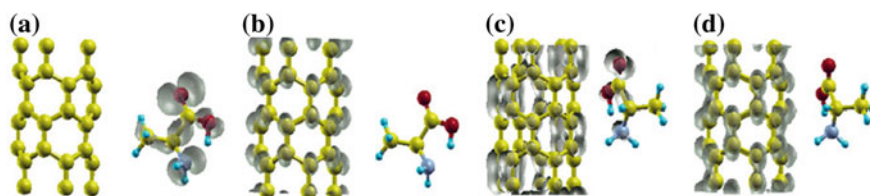
Fig. 9 Molecular modeling of interfacial interactions with a (5, 0) CNT [11]: **a** Highest occupied molecular orbital (HOMO) of a conformer $C_{50}ACH_3$-I (E = −0.12 eV). **b** Lowest unoccupied molecular orbital (LUMO) of a conformer $C_{50}ACH_3$-I (E = 0.38 eV). **c** The HOMO of a conformer $C_{50}ANH_2$-II (E = −0.23 eV). **d** The LUMO of a conformer $C_{50}ANH_2$-II (E = 0.25 eV)

interactions within the framework of registry potentials and the registry matrix analysis. Non-covalent interactions in the absorption of alanine onto a zig-zag (5, 0) carbon nanotube also occur within the lattice registry potentials, however, they are analyzed by the charge density analysis. In the highest occupied molecular orbital (HOMO) of the conformer $C_{50}ACH_3$-I (Fig. 9a), the charge is distributed over the alanine homogeneously. The resulting electrostatic interaction with carbon nanotube is one of the most stable among the conformers.

The covalent bonding illustrated in Fig. 10 [11] is associated with the so called perfect bonding or perfect adhesion in the classic micromechanics of composite

Fig. 10 Molecular modeling of covalent absorption [11]: **a–e** Covalent adsorption of alanine radicals onto a (5, 0) zig-zag carbon nanotube with **a** $C_{50}ANH$-I, **b** $C_{50}AN$-I, **c** $C_{50}AN$-II, **d** $C_{50}ACOO$-I and **e** $C_{50}ACO$-I

materials [1], which is examined in great details in chapter "Molecular Mechanics of Polymer Nanocomposites" of this edited volume. Molecular modeling, which is shown in Figs. 8, 9 and 10, and the examples included in the earlier editor's notes provide good illustrations for the molecular mechanics modeling of polymer nanocomposites [12–14] presented in chapter "Molecular Mechanics of Polymer Nanocomposites". The modeling techniques and the new research reviewed in chapter "Molecular Mechanics of Polymer Nanocomposites" are based on the powerful Monte Carlo methods.

References

1. V.M. Harik, *Mechanics of Carbon Nanotubes* (Nanodesigns Press, Newark, 2011)
2. X. Song, Q. Ge, S.C. Yen, An ab-initio study of mechanical behavior for $(AIO)_n$ nanorods, ed. by T. J. Chuang et al., in *Nanomechanics of Materials and Structures* (Springer, Berlin, 2006), pp. 23–32
3. W.J. Meng, G.Z. Voyiadjis, Structure and mechanical properties of ceramic nanocomposite coatings, Chapter 4 in *Trends in Nanoscale Mechanics* ed. by V.M. Harik, M.D. Salas (Kluwer Academic Publishers, The Netherlands, 2003), pp. 89–120
4. G.Z. Voyiadjis, E.C. Aifantis, G.Weber, Constitutive modeling of plasticity in nanostructured materials, Chapter 5 in *Trends in Nanoscale Mechanics* ed. by V.M. Harik, M.D. Salas (Kluwer Academic Publishers, The Netherlands, 2003), pp. 123–146
5. Z. Ounaies, C. Park, K.F. Wise, E.J. Siochi, J.S. Harrison, Electrical properties of single wall carbon nanotube reinforced polyimide composites. Compos. Sci. Technol. **63**, 1637–1646 (2003)
6. S. Stankovich, D.A. Dikin, G.H.B. Dommett, K.M. Kohlhaas, E.J. Zimney, E.A. Stach, R.D. Piner, S.B.T. Nguyen, R.S. Ruoff, Graphene-based composite materials. Nature **442**(20), 282–286 (2006)
7. C.Y. Li,T.-W. Chou, Multiscale modeling of the interfacial load transfer in carbon nanotube/ polymer composites, J. Nanosci. Nanotech. **3**, 423–430 (2004)
8. S.J.V. Frankland, V.M. Harik, Surf. Sci. Lett. **525**, L103–L108 (2003)
9. S.K. Yadav, S.S. Mahapatra, J.W. Cho, H.C. Park, J.Y. Lee, Fibers Polym. **10**(6), 756–760 (2009)
10. L. Gao, L. Jiang, J. Sun, J. Electroceram. **17**, 51–55 (2006)
11. M. Rajarajeswari, K. Iyakutti, Y. Kawazoe, J. Mol. Model. **18**, 771–781 (2012)
12. C.Y. Li, T.-W. Chou, Modeling of carbon nanotubes and their composites, in *Nanomechanics of Materials and Structures*, ed. by T.J. Chuang et al. (Springer, Berlin, 2006), pp. 55–65
13. S.J.V. Frankland, V.M. Harik, Mat. Res. Soc. Symp. Proc. **733 E**, T6.2.1 (2002)
14. V.M. Harik, R.A. Cairncross, Mech. Mater. **32**, 807 (2000)